Energy Proceedings
Vol 44, 2024
ISSN 2004-2965

# Eco-Building Materials: Metakaolin-based Geopolymer for CO2 Emission Reduction and Enhanced Energy Efficiency

Yifan Zhou[1], Junwei Liu[2*], Jinyue Yan[2*]

1 College of Civil Engineering and Architecture, Zhejiang University, Hangzhou, China

2 Department of Building Environment and Energy Engineering, International Centre of Urban Energy Nexus, The Hong Kong Polytechnic University, Kowloon, Hong Kong, China
(*Corresponding Author: jwliu628@tju.edu.cn)

**ABSTRACT**

Considering diminishing limestone resources and escalating carbon emission regulations, geopolymers are considered to be the third generation of cementitious materials after lime and ordinary Portland cement (OPC). Geopolymers are distinguished by their strong corrosion resistance, freeze-thaw resilience, mechanical strength, and reduced $CO_2$ emissions, positioning them as environmentally friendly alternatives to traditional cement. Metakaolin (MK) based geopolymers typically have a light-colored appearance which contributes to high solar reflectance, thereby reducing heat absorption from sunlight and rendering them beneficial for radiative cooling. Enriched with alumina ($Al_2O_3$) and silicon dioxide ($SiO_2$), MK geopolymers possess unique radiative properties, outperforming in radiative cooling experiments with a notable temperature drop of about 6.5˚C. Compared to other green alternatives like slag and fly ash geopolymers, MK geopolymers demonstrate enhanced strength and thermal stability. A life cycle assessment reveals that metakaolin-based geopolymers can mitigate carbon emissions compared to ordinary Portland cement (OPC), underscoring their role as a sustainable solution in the construction industry.

**Keywords:** Eco-building materials, Geopolymers, Radiative cooling, Energy saving, Mechanical properties.

**NONMENCLATURE**

| | |
|---|---|
| *Abbreviations* | |
| OPC | Ordinary Portland Cement |
| MK | Metakaolin |
| SDRCC | Sub Environmental Daytime Radiation-cooled Coating |
| PGEO | Phosphoric Acid-based Geopolymer |
| TGA | Thermogravimetric Analysis |
| LCA | Life Cycle Assessment |
| XRD | X-Ray Difffraction |
| *Symbols* | |
| $R_c$ | Compressive Strength |
| $F_c$ | Compressive Force |
| A | Area |
| $\theta$ | Diffraction Half Angle |

## 1. INTRODUCTION

### *1.1 Reduced carbon footprint in production*

The production of traditional Portland cement (OPC) is a significant contributor to global carbon emissions, accounting for approximately 8% of the total [1]. This is primarily attributed to the energy-demanding calcination of limestone and the operations of high-temperature kilns. In the pursuit of more sustainable construction materials, geopolymers have been highlighted as alternatives for the utilization of industrial wastes such as fly ash, slag, and kaolinite. Emerging research [2] [3] on geopolymers and alkali-activated materials has indicated that metakaolin-based geopolymers might offer a viable alternative to OPC in certain applications.

Metakaolin stands out as a unique supplementary cementitious material. Unlike typical industrial by-products or natural materials, metakaolin is a dehydroxylated form of the clay mineral, kaolinite. This material is primarily obtained by calcining kaolin clays between temperatures of 600°C to 900°C. This calcination not only refines the color and removes inert

# This is a paper for 15th International Conference on Applied Energy (ICAE2023), Dec. 3-7, 2023, Doha, Qatar.

impurities but also optimizes its particle size [3]. As articulated in Equation:

$$Al_2Si_2O_5(OH)_4 \rightarrow Al_2O_3 \cdot 2SiO_2 + 2H_2O\uparrow$$

The conversion to metakaolin occurs at relatively lower temperatures and results in the release of water rather than carbon dioxide, which contrasts with conventional cement processes.

According to Ababneha's research [4], a specific proportion of kaolin-based cement incurs a cost and energy content that are 45% and 70% less than Portland cement, respectively, underscoring its potential to revolutionize the construction industry in an eco-friendly manner.

Moreover, metakaolin-based geopolymers are known for their enhanced resistance to corrosion, freeze-thaw cycles, and certain chemical attacks. This durability means structures made from these materials may have a longer lifespan, reducing the frequency of replacements and the associated energy and emissions from production.

### *1.2 Thermal insulation properties*

The energy consumption of the commercial building sector represents a significant portion, accounting for about 42% of the total energy consumption across primary sectors like industry, transportation, and agriculture [5]. As a result, the spotlight has increasingly focused on the role of thermal insulation in enhancing energy efficiency in buildings, given its capacity to reduce energy losses. Achieving optimal thermal conductivity, which would effectively reduce energy consumption, often requires the composite of various materials.

Geopolymers have emerged as a promising alternative in this context. The thermal properties of geopolymers are influenced by their nominal composition, gel phase short-range ordering, interconnectivity, and pore distribution [6]. Due to its relatively consistent chemical composition and insulation properties compared to materials like slag or fly ash, Metakaolin has become the preferred source for producing insulating geopolymers [7].

Significant research has been undertaken to understand and optimize the thermal properties of metakaolin-based geopolymers. Kamseu et al. [8] achieved thermal conductivity values between 0.3 and 0.59 W/m using MK-based geopolymer activated with a combination of NaOH, KOH, and sodium silicate solution. Rashad [9] explored the use of expanded perlite and natural sand as fine aggregates, achieving thermal conductivities of 0.6 and 0.93 W/m K, respectively. Other studies [10] [11] have also demonstrated promising results, with thermal conductivities in the range of 0.55-0.65 W/m K and 0.466-0.66 W/m K, respectively, using different formulations and activating solutions.

### *1.3 Potential radio cooling properties*

A feature of these geopolymers is their light coloration, which contributes to a high solar reflectance. The solar reflectance of metakaolin-based geopolymer is considerably high, exceeding 70% [12]. This inherent property not only aids in mitigating the urban heat island effect but also reduces the dependency on air conditioning in buildings, making it suitable for sub environmental daytime radiation-cooled coating (SDRCC) applications, consequently improving energy performance. In practical applications [12], this specifically formulated coating showcased an infrared emissivity of 0.9491 coupled with a solar reflectance of 97.6%. Under the climatic conditions of Hong Kong, when subjected to direct sunlight, the coating's surface displayed an ability to cool down by a remarkable 8.9˚C below the surrounding air temperature.

Incorporating another dimension to this exploration is the introduction of Phosphoric acid-based geopolymer (PGEO), a unique aluminosilicate inorganic polymeric material. PGEO is synthesized by activating aluminosilicate precursors, such as metakaolinite, in a phosphoric acid solution, leading to a three-dimensional network comprising −Si−O−Al−O−P−O− structures [13]. This intricate matrix amalgamates several infrared active groups, facilitating an expanded range of infrared radiation. Furthermore, the inherent network structures of PGEO ensure electrical neutrality, thanks to the charge-balancing mechanism that minimizes the ion polarization effect, thereby moderating the infrared extinction coefficient [14].

Chen et al. [15] used metakaolin to form a new coating that boasts of exceptional spectral selectivity, evidenced by an average infrared emissivity of approximately 0.95 and a solar light reflectivity surpassing 0.90 with a significant temperature drop of about 8.3°C during midday. Moreover, when compared with conventional organic polymer-based daytime radiative cooling materials, this innovative inorganic paint displays heightened resistance to factors like mechanical abrasion, heat, and proton irradiation.

In conclusion, the development and adoption of metakaolin-based geopolymers represent a multi-faceted approach to enhancing energy performance in mitigating CO2 emissions and the built environment. From production to end-use, these materials offer a

more sustainable alternative to conventional construction materials like Portland cement.

## 2. MATERIALS AND METHODS

### *2.1 Preparation of metakaolin-based geopolymer*

Metakaolin, derived from natural kaolin, is altered by high-temperature treatments, leading to irregular molecular structures and significant reactivity. With low calcium and rich silicon and aluminum oxides content, metakaolin is a suitable material for geopolymer synthesis, as the components shown in Table 1.

Table 1. XRF of metakaolin

| $SiO_2$ | $Al_2O_3$ | $Fe_2O_3$ | $K_2O$ | $TiO_2$ |
|---|---|---|---|---|
| 52.7500% | 45.2500% | 1.3250% | 0.6975% | 0.2438% |

Alkaline activators in the preparation of geopolymers usually use alkaline silicate solutions. It provides an alkaline environment and supply free silicic acid and water essential for polymerization. These activators are typically modified water glass with sodium hydroxide, with specific proportions outlined in Table 2.

Table 2. Proportions of alkaline activator

| Sodium silicate | NaOH | $H_2O$ | Modulus ($SiO_2/Na_2O$) |
|---|---|---|---|
| 1 | 0.22 | 1.76 | 1.51 |

The proper proportion of metakaolin-based polymer paste was identified through experiments, with the final ratio provided in Table 3.

Table 3. Paste ratio for the metakaolin-based geopolymer paste

| MK | Alkali activator | Water content ($m_{water}/m_{total}$) | AE% | Si/Al |
|---|---|---|---|---|
| 1 | 1.4 | 34.21% | 21.53 | 1.5 |

### *2.2 Radiative cooling*

Radiative cooling experiments are carried out on the roof of the 43rd academic building in Tianjin University (Tianjin, China) and the experimental devices including radiative coolers are placed on the support 1 m above the ground, as shown in Figure 1. The device is placed on the surrounding roof without any shelter, K-type thermocouples with an error of ±0.3 °C are calibrated prior to use. The data logger is adopted to record the radiative cooler temperature every 2 minutes and the meteorological data during the experiment are collected by the small meteorological station, including the ambient temperature, dew point temperature, humidity, wind speed and solar radiation.

The radiative cooling experiment in this paper was conducted in Tianjin, China on September 29, which was a sunny day, suitable for the development of radiative cooling experiment.

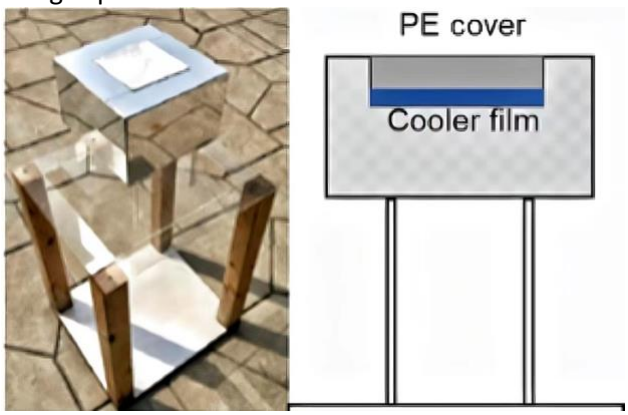


Fig. 1. Experimental device for radiative cooling performance

### *2.3 Mechanical properties*

Specimens with prismatic shapes, measuring 40×40×160 mm, were utilized to assess the mechanical attributes of the mortars. They were maintained in a standard curing environment at a temperature of 20 ± 2 °C and over 90% relative humidity. After a period of 24 ± 2 hours, these samples were removed from their molds and stored under the same environmental conditions.

Compressive strength Rc (MPa) was calculated using Equation (1).

$$R_c = \frac{F_c}{A} \quad (1)$$

In the above equation, $F_c$ is the maximal load at the time of damage (N) and A is the compressed area (1600 $mm^2$). For strength tests, for each age period, six specimens of each mortar mix were tested in parallel experiments.

### *2.4 Thermal stability*

Thermogravimetric Analysis (TGA) tests were performed using a Q50 TG analyzer (TGA). The specimens for the TGA tests were subjected to the termination of hydration and drying, i.e., the specimens were placed in anhydrous ethanol to terminate hydration immediately after the compressive strength test, and then placed in an oven at 60 °C for 48 h before the TGA tests. The dried specimens were ground to a fine powder, with particle sizes under 0.08 mm. Ten to fifteen milligrams of the specimen were heated from 20 to 1000 °C, at a heating rate of 10 °C/min, under a gaseous nitrogen flow. The TG tests were conducted at a single point for each sample.

### *2.5 Life cycle carbon emission assessment*

In this study, we focus on the evaluation of CO2 emissions associated with the production of kaolin-based cement, employing Life Cycle Assessment (LCA) as

a principal analytical tool to quantify the environmental performance throughout its life cycle. An analysis encompassing the extraction, processing, and utilization stages is presented, with a particular emphasis on the reduction of carbon emissions as compared to traditional Portland cement. We provide an assessment of carbon emissions originating from diverse processes involved in the production of metakaolin-based geopolymer.

## 3. RESULTS AND DISCUSSION

### *3.1 Production*

The component crystal pattern of metakaolin-based geopolymer after 28 days of polymerization is shown in Figure 2 below.

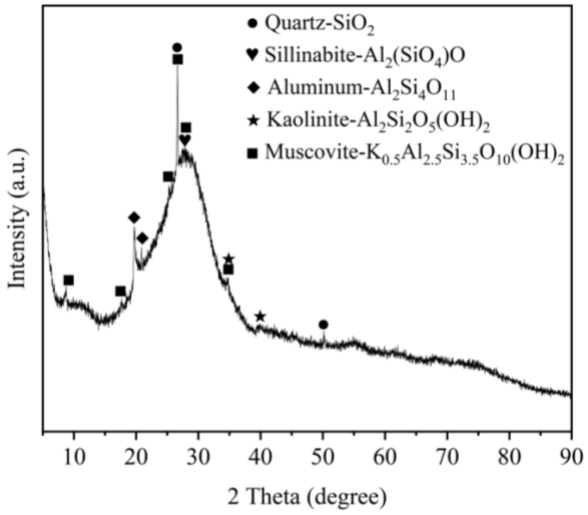


Fig. 2. XRD pattern of metakaolin-based geopolymer

After polymerization, the XRD pattern of metakaolin-based geopolymer exhibited the characteristic of amorphous structure, indicated by a broad diffraction hump spanning 20° to 35° (2θ). This dispersion peak, attributable to the amorphous aluminosilicate gel, aligns with the findings of Palomo et al. and Rahier et al. [16,17].

Despite the polymerization process, distinctive diffraction peaks of quartz persist. This retention implies quartz's non-participation in the polymerization, attributed to its low dissolution propensity in alkaline media [18, 19]. The transformation within the amorphous structure of metakaolin, however, fostering a continual augmentation in the geopolymer's compressive strength over time [20].

Delving into the polymerization mechanics, it is a coordinated play of solid reactants' dissolution, dissolved species' transition to the gel phase, nucleation, and the gel phase's condensation. The alkali activator facilitates the dissolution of solid raw material particles, yielding a reactive, soluble concoction rich in Si and Al, forming the tetrahedral aluminosilicate units [21]. Concurrently, the soluble silicate accelerates the polymerization, offering self-polymerizing species and instigating the polymerization among silicate oligomers and the derived tetrahedral aluminosilicate units. The production of this intricate process manifests as an amorphous structure [22].

### *3.2 Radiative Cooling*

In the environment of Tianjin on September 29, the cooling performance of metakaolin-based geopolymers and the ambient temperature and relative humidity are shown in Figure 3 below.

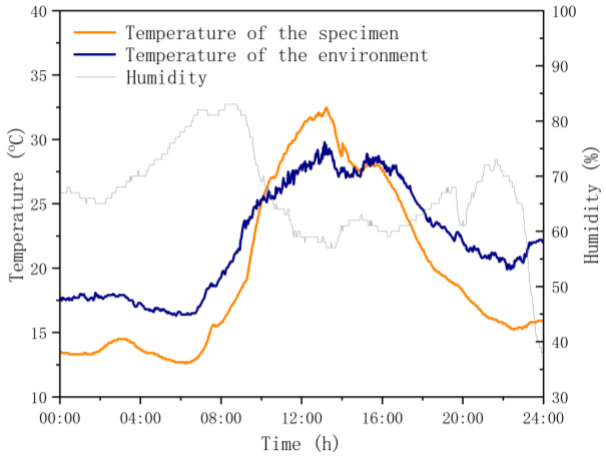


Fig. 3. Radiative cooling performance

According to Figure. 3, it is observed that the temperature of the test block within the experimental apparatus fluctuates in response to changes in ambient temperature. Remarkably, for nearly 80% time of the day, the temperature of the emitter is lower than the environment temperature, with the maximum temperature difference of about 6.5℃ occurring between 22:00 and 23:00 at night. This can be attributed to the reduced wind speed and absence of solar radiation absorption at night, leading to an increased net radiative cooling power. This pattern underscores the efficacy of radiative cooling in reducing indoor temperatures and, by extension, diminishing the cooling load that air conditioning systems must handle.

However, a distinct shift is observed during the noon period of 10:00 to 14:00, where the temperature of the test block approaches or even surpasses the ambient temperature, with a maximum excess of 1.7˚C. This temperature rise is attributed to the amplified solar radiation in these peak hours, which, in combination with a persistent relative humidity exceeding 55% and a

low wind speed, undermines the test block's cooling efficiency. In this midday period, the environment's thermodynamic conditions are not conducive for the block to radiate the absorbed heat effectively, leading to a reduction in its radiant cooling capacity. This observation underscores an evident need for implementing adaptive cooling methodologies.

### *3.3 Mechanical Properties*

The following figure shows the strength of various geopolymers and ordinary Portland cement.

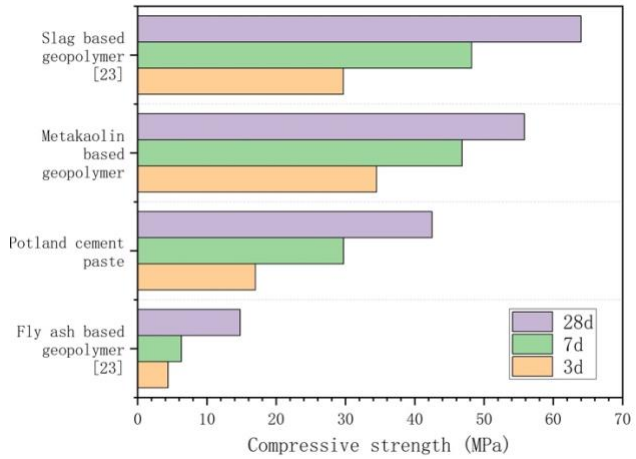


Fig. 4. Compressive strength of different materials

From the analysis of both experimental and literature data, trends emerge in the comparative strength of metakaolin-based geopolymers, slag-based geopolymers, and fly ash-based geopolymers, as depicted in the above figure. While the actual strength of each type of geopolymer is influenced by variables including preparation method, polymerization, and curing conditions, the results offer insights into the mechanical properties of these materials.

In the case of fly ash-based geopolymers, the lower strength is linked to its reduced reaction activation, a consequence of its limited content of reactive silicate and aluminate. This deficiency culminates in a less dense and weaker geopolymer network structure, resulting in compromised strength.

The strength of metakaolin-based polymer and slag-based geopolymer is relatively strong. Both are higher than ordinary Portland cement. In terms of long-term strength, slag-based geopolymers slightly outperform, while metakaolin geopolymers exhibit superior early strength. This can be attributed to the microstructure of metakaolin, which is denser and more uniform, contributing to the material's enhanced initial strength. Conversely, the chemical composition and microstructure of slag are more complex, resulting in reduced reactivity and curing speed compared to metakaolin. The slag-based geopolymer requires an extended duration to fully develop and optimize its microstructure and mechanical properties. Therefore, metakaolin-based geopolymer, characterized by its pure and stable composition, possesses certain strength advantages.

### *3.4 Thermal stability*

The TG-DTG curves of metakaolin-based geopolymer are shown in Figure 5.

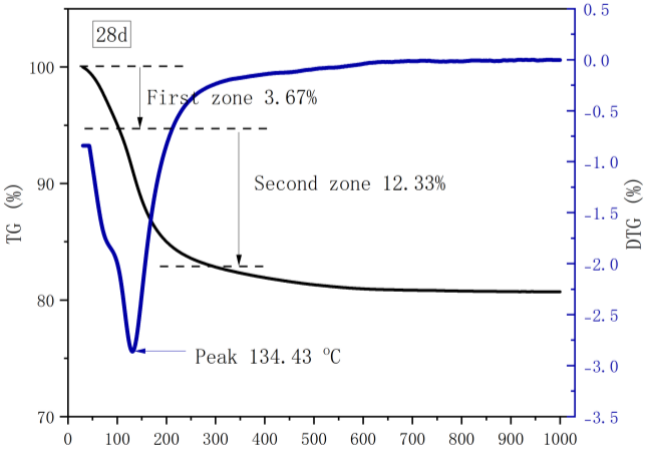


Fig. 5. TG and DTG curves of metakaolin-based geopolymer

Based on the research by Bell and Duxson [24], the thermal stability of geopolymers is categorized into four distinct zones, each characterized by specific thermal behaviors. In the first zone, below 100˚C, mass loss is attributed to the evaporation of free water contained within the sample. The second zone, ranging from 100-300˚C, sees the loss of bound water, a byproduct of T-OH polymerization, along with a minor reduction attributed to zeolite content. The third and fourth zones span the temperature ranges of 300-700˚C and 700-1000˚C, respectively. Mass loss within these ranges is predominantly due to capillary and physical concentration instigated by the polymerization of -OH groups and the sintering of viscous substances. Moreover, the decomposition of carbonates, arising from efflorescence, also contributes to mass loss in these zones.

Compared with the figure above, the TG-DTG curves of slag-based geopolymer [25] and fly ash-based geopolymers [26] show weight losses at 300-700˚C and 700-1000˚C, except for the peaks at about 100 ° C. The mass loss that occurred in the range from 300 to 700 °C was caused by the dehydroxylation and dehydration of the geopolymer structure. The small DTG peaks approximately at 700 °C–1000 °C were due to the decomposition of calcite ($CaCO_3$) to carbon-di-oxide

($CO_2$) [27]. As a result, metakaolin usually contains purer silicates and aluminates, which may show better stability for its geopolymer at high temperatures.

### *3.5 Water resistance*

The TG-DTG curves of metakaolin-based geopolymer are shown in Figure 5.

The waterproofing characteristics of building materials are an essential factor in construction. Traditional cementitious material such as OPC typically exhibits high hydrophilicity due to its porous structure and chemical composition, which facilitates moisture absorption. In this study, contact angle experiments were conducted to compare the hydrophobic properties of metakaolin-based geopolymers, OPC, and wood. The results are presented in the following figures.

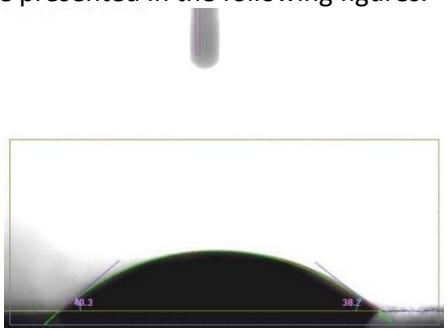

(a) Geopolymer $\alpha = 39.3°$

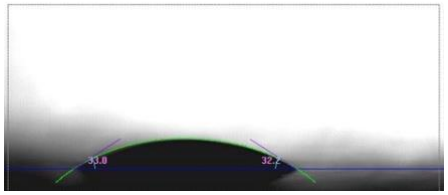

(b) Ordinary Portland cement $\alpha = 32.6°$

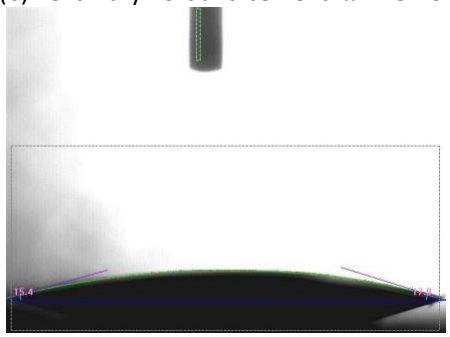

(c) Wood $\alpha = 16.2°$

Fig. 6. Contact angles

The results depicted that all three materials exhibit relative hydrophilicity. However, the geopolymers demonstrate a larger contact angle, suggesting a comparatively enhanced hydrophobic effect.

Research has shown that appropriate treatments can enhance the hydrophobic properties of geopolymers. For instance, silane modification has been found to confer surface hydrophobicity to geopolymers. [28] This modification effectively reduces water capillary absorption and outward moisture diffusion, consequently diminishing the leaching of soluble alkali ions. Furthermore, a novel surface waterproof geopolymer, developed through alkali activation of metakaolin and a hydrophobic modification agent, demonstrated a significant increase in contact angle from 36° to 132°. [29] Enhanced hydrophobic properties can broaden the range of applications for polymers.

### *3.6 Life cycle carbon emission assessment*

Specific metakaolin-based geopolymer life cycle carbon factors need to be analyzed and processed according to a more adequate database. At present, we can draw the following results from previous studies.

Metakaolin-based geopolymers generally exhibit lower carbon emissions compared to traditional Portland cement [4]. Raw material extraction and processing should be a key factor.

The thermal energy process was added to the kaolin process to depict the energy required for calcining kaolin into metakaolin. The thermal energy required was 2.5 MJ/kg [30]. Tasiopoulou [31] evaluated the effect of various operational parameters and scenarios, such as calcination temperature, moisture and drying of raw material, exhaust gas recirculation and the use of alternative-fuel combustion (to provide a heat requirements). Exhaust gas recirculation (EGR) can lead to average energy savings of up to 38%. Contrastingly, the manufacture of Portland cement is notably energy-intensive, characterized by the heating of limestone and assorted materials to approximately 1450°C. This method is not only energy exhaustive but is also a significant source of carbon dioxide emissions.

In terms of durability of use, metakaolin-based geopolymers have excellent durability and enhanced resistance to chemical corrosion. These traits contribute to their reduced need for maintenance, repair, and replacement, leading to lower emissions over their lifespan.

Furthermore, the potential for integrating metakaolin with industrial by-products, like slag and fly ash, to form compound geopolymers [32], amplifies its environmental benefits.

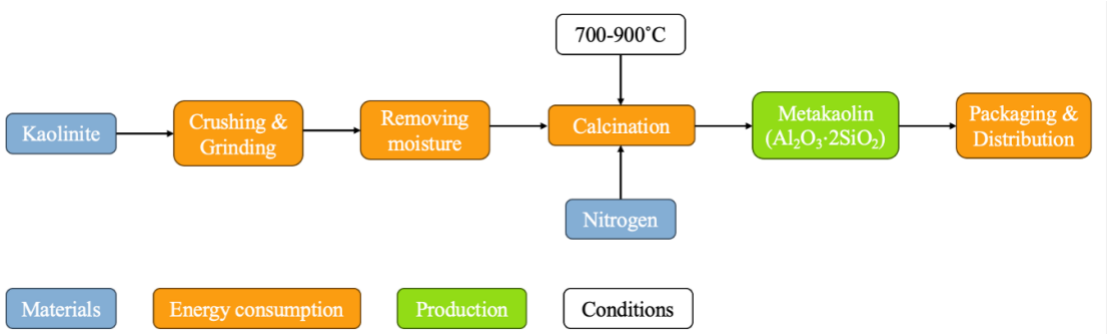

Fig. 7. The life-cycle boundary of metakaolin

## 4. CONCLUSIONS

(1). Metakaolin-based geopolymers exhibit relatively good cooling radiation functionality, capable of achieving a temperature approximately 6.5°C lower than the environment surroundings at their peak efficiency. However, enhancing this cooling effect during noon hours necessitates design improvements.

(2). Metakaolin-based geopolymers have enhanced mechanical properties in comparison to other green geopolymers attributed to their more uniform and dense chemical composition.

(3). The thermal stability of metakaolin-based geopolymers outperforms that of other green geopolymers.

(4). A reduction in carbon emissions is achievable with the application of metakaolin-based geopolymers in the building materials industry, compared to traditional cement.

## REFERENCE

[1] [1] Van der Geer J, Hanraads JAJ, Lupton RA. The art of Miller, S. A., Horvath, A., & Monteiro, P. J. M. (2016). Readily implementable techniques can cut annual CO2 emissions from the production of concrete by over 20%. Environ. Res. Lett., 11, 074029.

[2] Abiodun, Y.O., Sadiq, O.M., Adeosun, S.O., & Oyekan, G.L. (2019). Mineralogical Properties of Kaolin and Metakaolin from Selected Areas in Nigeria and Its Application to Concrete Production. West Indian J. Eng., 42, 57–64.

[3] Biljana, R., Alexandra, A., & Ljiljana, R. (2010). Thermal Treatment of Kaolin Clay to Obtain Metakaolin. Institute for Testing of Materials: Belgrade, Serbia, 64, 351–356.

[4] Ayman Ababneha, Faris Matalkahb, & Ruba Aqelb. (2020). Synthesis of kaolin-based alkali-activated cement: carbon footprint, cost and energy assessment. Journal of Materials Research and Technology, 9(4), 8367–8378.

[5] Ruellan, M., Park, H., & Bennacer, R. (2016). Residential building energy demand and thermal comfort: Thermal dynamics of electrical appliances and their impact. Energy Build., 130, 46–54.

[6] Villaquirán-Caicedo, M.A., de Gutiérrez, R.M., Sulekar, S., Davis, C., & Nino, J.C. (2015). Thermal properties of novel binary geopolymers based on metakaolin and alternative silica sources. Appl. Clay Sci., 118, 276–282.

[7] Rashad, A.M. (2017). Possibility of using metakaolin as thermal insulation material. Int. Thermophys., 38(126), 1–11.

[8] Kamseu, E., Ceron, B., Tobias, H., Leonelli, E., Bignozzi, M.C., Muscio, A., & Libbra, A. (2012). Insulation behavior of metakaolin-based geopolymer materials assess with heat flux meter and laser flash techniques. J. Therm. Anal. Calorim., 108, 1189–1199.

[9] Rashad, A.M. (2019). Insulating and fire-resistant behaviour of metakaolin and fly ash geopolymer mortars. Proc. Inst. Civ. Eng., 172(1), 37–44.

[10] Subaer, & van Riessen, A. (2007). Thermo-mechanical and microstructural characterisation of sodium-poly(sialate-siloxo) (Na-PSS) geopolymers. J. Mater. Sci., 42, 3117–3123.Samal

[11] Sneha, Thanh Nhan, Petrìková, I., Marvalová, B., Vallons, A.M.K., & Lomov, S.V. (2015). Correlation of microstructure and mechanical properties of various fabric reinforced geo-polymer composites after exposure to elevated temperature. Ceramic Int., 41, 12115-12122.

[12] Yang, N., Fu, Y., Xue, X., Lei, D., & Dai, J.-G. (2023). Geopolymer-based sub-ambient daytime radiative cooling coating. Eco. Mat., 5(2), e12284.

[13] Katsiki, A. (2019). Aluminosilicate phosphate cements: A critical review. Advances in Applied Ceramics, 118, 274-286.
[14] Cui, X.-m. , Liu, L.-p. , He, Y., Chen, J.-y. , & Zhou, J. (2011). A novel aluminosilicate geopolymer material with low dielectric loss. Materials Chemistry and Physics, 130, 1-4.
[15] Chen, G., Wang, Y., Qiu, J., Cao, J., Zou, Y., Wang, S., Jia, D., & Zhou, Y. (2020). Robust inorganic daytime radiative cooling coating based on a phosphate geopolymer. ACS Applied Materials & Interfaces, 12(49), 54963-54971.
[16] Palomo, A.; Glasser, F.P. Chemically-bonded cementitious materials based on metakaolin. Br. Ceram. Trans. J. 1992, 91, 107–112.
[17] Rahier, H.; Mele, B.B.; Biesemans, M.; Wastiels, J.; Wu, X. Low-temperature synthesized aluminosilicate glasses. J. Mater. Sci. 1996, 31, 71–79.
[18] Choquette, M.; Berube, M.A.; Locat, L. Behaviour of common rock-forming minerals in a strongly basic NaOH solution. Can. Mineral. 1991, 29, 163–173.
[19] Palmero, P.; Formia, A.; Antonaci, P.; Brini, S.; Tulliani, J.-M. Geopolymer technology for application-oriented dense and lightened materials. Elaboration and characterization. Ceram. Int. 2015, 41, 12967–12979.
[20] hang, S.Z.; Gong, K.C. Geopolymer. Mater. Sci. Eng. 2003, 3, 430–436.
[21] Williams, R.P., Hart, R.D., & van Riessen, A. (2011). Quantification of the extent of reaction of metakaolin-based geopolymers using X-ray diffraction, scanning electron microscopy, and energy-dispersive spectroscopy. Journal of the American Ceramic Society, 94(9), 2663-2670.
[22] Subaer, A. van Riessen, B. H. O'Connor, and C. E. Buckley, Compressive Strength and Microstructural Character of Aluminosilicate Geopolymers, J. Australas. Ceram. Soc., 38 [1] 83–6 (2002).
[23] Kriven, W. M., Wang, J., Zhu, D., & Fischer, T. (2015). Long-term development of mechanical strengths of alkali-activated metakaolin, slag, fly ash, and blends. 39th International Conference on Advanced Ceramics and Composites, pp. 77–87.
[24] Duxson, P., Lukey, G. C., & van Deventer, J. S. J. (2006). Thermal evolution of metakaolin geopolymers: Part 1 – Physical evolution. Journal of Non-Crystalline Solids, 352(52–54), 5541-5555.
[25] Karthik, A., Sudalaimani, K., Vijayakumar, C. T., & Saravanakumar, S. S. (2019). Effect of bio-additives on physico-chemical properties of fly ash-ground granulated blast furnace slag based self cured geopolymer mortars. Journal of Hazardous Materials, 361, 56-63.
[26] Pu, S., Zhu, Z., Song, W., Huo, W., & Zhang, J. (2021). Mechanical and microscopic properties of fly ash phosphoric acid-based geopolymer paste: A comprehensive study. Construction and Building Materials, 299, 123947.
[27] Thirumalini, S., Ravi, R., Sekar, S. K., & Nambirajan, M. (2015). Knowing from the past – ingredients and technology of ancient mortar used in Vadakumnathan temple, Tirussur, Kerala, India. Journal of Building Engineering, 4, 101-112.
[28] Xue, X., Liu, Y.-L., Dai, J.-G., Poon, C.-S., Zhang, W.-D., & Zhang, P. (2018). Inhibiting efflorescence formation on fly ash–based geopolymer via silane surface modification. Cement and Concrete Composites, 94, 43-52.
[29] Duan, P., Yan, C., Luo, W., & Zhou, W. (2016). A novel surface waterproof geopolymer derived from metakaolin by hydrophobic modification. Materials Letters, 164, 172-175.
[30] Munir, Q., Abdulkareem, M., Horttanainen, M., & Kärki, T. (2023). A comparative cradle-to-gate life cycle assessment of geopolymer concrete produced from industrial side streams in comparison with traditional concrete. Science of The Total Environment, 865, 161230.
[31] Tasiopoulou T, Katsourinis D, Giannopoulos D, Founti M. Production-Process Simulation and Life-Cycle Assessment of Metakaolin as Supplementary Cementitious Material. Eng. 2023; 4(1):761-779.
[32] Wang A, Fang Y, Zhou Y, Wang C, Dong B, Chen C. Green Protective Geopolymer Coatings: Interface Characterization, Modification and Life-Cycle Analysis. Materials. 2022; 15(11):3767.